Catal Lett (2011) 141:1136–1141
DOI 10.1007/s10562-011-0580-8

# Synthesis of Nanosized AlKIT-1 Mesoporous Molecular Sieve and its Catalytic Performance for the Conversion of 1,2,4-Trimethylbenzene

**Liping Liu · Guang Xiong · Xiangsheng Wang · Xiaojing Cheng**

Received: 10 January 2011 / Accepted: 9 March 2011 / Published online: 19 March 2011


**Abstract** Nanosized mesoporous AlKIT-1 molecular sieve was hydrothermally synthesized in the absence of organic salts. The samples were characterized by X-ray diffraction, electron microscopy (TEM and SEM), $N_2$ adsorption isotherm, and $NH_3$-TPD methods. The AlKIT-1 has a particle size of about 60–100 nm, and a three-dimensional network structure with average pore size of 2.7 nm. The sample exhibits good hydrothermal stability and catalytic performance for 1,2,4-trimethylbenzene, suggesting its promising applications in the conversion of large molecules.

**Keywords** Nanosized AlKIT-1 mesoporous molecular sieve · Hydrothermal stability · 1,2,4-Trimethylbenzene

## 1 Introduction

Since the discovery of M41S molecular sieves, varied kinds of mesoporous materials with large surface area and uniform pore channels have been synthesized, e. g., HMS, MSU, KIT-1, SBA-15 [1–5]. KIT-1 is a three-dimensional mesoporous molecular sieve with uniform pore size and high surface area. In particular, the disordered KIT-1 is hydrothermally more stable than ordered MCM-41. The KIT-1 is generally synthesized by an electrostatic templating route using sodium silicate, HTAC1, and ethylenediaminetetraacetic acid tetrasodium salt ($EDTANa_4$) [4]. The catalytic activity of the material was investigated for Friedel–Crafts alkylation of benzene, toluene, and m-xylene by using benzyl alcohol as the alkylation agent [6]. Zhao et al. [5] synthesized disordered mesoporous aluminosilicates (DMASs), which are similar to mesoporous KIT-1 [7]. The resulting materials show higher hydrothermal stability, surface acid strength and cracking activities than Al-MCM-41. KIT-1 supported $MoO_3$ and/or NiO catalysts exhibit higher catalytic activities for thiophene hydrodesulfurization than MCM-41 and NaY zeolite supported catalysts [8]. Therefore, KIT-1 shows promising applications for catalytic conversion of large molecules.

In recent years nanosized zeolites have drawn much attention due to their unique properties and catalytic performances [9–11]. Particle size reduction decreases the molecular diffusion paths and increases the external surface area, thus limits the coke formation and improves catalytic properties. Most studies focus on the synthesis and application of nanosized ZSM-5, Y etc. To the best of our knowledge, the synthesis of nanosized mesoporous AlKIT-1 has not been reported.

In this article, we report a simple synthesis procedure to directly synthesize hydrothermally stable, nanosized AlKIT-1 molecular sieves. Organic salts ($EDTANa_4$, sodium salicylate, sodium salts adipic acid, and sodium salts benzenedisulfonic acid) or polymer aluminosilicate precursors are not required to obtain the disordered three-dimensional structure. The catalytic performance of the resulting material was tested by the conversion of 1,2,4-trimethylbenzene. The reaction results of the nano-AlKIT-1 were compared with those of HMCM-41 and HZSM-5.

L. Liu · G. Xiong (✉) · X. Wang · X. Cheng
State Key Laboratory of Fine Chemicals, Department of Catalytical Chemistry and Engineering, Dalian University of Technology, Dalian 116024, Liaoning, People's Republic of China
e-mail: gxiong@dlut.edu.cn

X. Cheng
School of Chemistry and Chemical Engineering, Xinjiang University, Urumqi 830046, People's Republic of China

## 2 Experimental

### 2.1 Synthesis of Nanosized AlKIT-1

Chemical reagents included sodium aluminum ($NaAlO_2$) (AR, Tianjin Chemical Reagent Institute), tetraethylorthosilicate (TEOS), cetyltrimethylammonium bromide (CTAB) (AR, Tianjin Guangfu Fine Chemical Research Institute), and ammonia (AR, Shenyang Lianbang Reagent Institute).

The nanosized AlKIT-1 were synthesized as follows: 4.87 g of CTMABr and 120 g of water were mixed and stirred for 10 min. Thereafter, 0.18 g of sodium aluminate was added to the surfactant solution with vigorous stirring. After stirring for 30 min, 14.3 g of TEOS was added to the synthesis mixture and the resulting gel was stirred at room temperature for 4 h. The ammonia was added dropwise to the above mixture to increase the pH to 10.5, and then stirred for 2 h. The molar composition is $86SiO_2$: $Al_2O_3$: 17.2CTAB: $8600H_2O$. The homogeneous gel was transferred to a 200 $cm^3$ teflon-lined stainless steel autoclaves and heated for 48 h at 120 °C. The solid was filtered and washed with deionized water, dried at 100 °C and then calcined in air at 550 °C for 6 h. The calcined product is finally ion-exchanged by stirring in 0.4 M $NH_4NO_3$ for 6 h (three times) and subsequently washed and dried at 100 °C. The product was further calcined at 540 °C for 4 h.

### 2.2 Characterization

X-ray powder diffraction (XRD) patterns were taken on a Rigaku D/Max 2400 diffractometer (Shimadzu Co.) using nickel-filtered CuKa X-ray source at a scanning rate of 0.02 over the range between 1.0 and 40°.

Transmission electron microscopy (TEM) images were recorded on a JEM-100CXII electron microscope operating at 200 kV. Samples for analysis were suspended and dispersed on a grid.

Scanning electron microscopy (SEM) images were recorded using a Hitachi S-4800 with an acceleration voltage of 15 kV. The samples were mounted using a conductive carbon double-sided sticky tape. A thin coating of gold sputter was deposited onto the samples to reduce the effects of charging.

$N_2$ adsorption and desorption isotherms were obtained using a Quantachrome AUTOSORB-1-MP apparatus at liquid nitrogen temperature. The samples were degassed at 350 °C prior to analysis. The mesoporous structure was determined from the adsorption branch of isotherms by using the Barrett–Joyner–Halenda (BJH) model. The microporous distribution was calculated by using HK model. The BET specific surface area of mesoporous sieves and zeolite were calculated from adsorption branch in the relative pressure range 0.05–0.2 and 0.05–0.1, respectively. The total pore volume was estimated from the amount adsorbed at a relative pressure of 0.99.

The $NH_3$ temperature programmed desorption ($NH_3$-TPD) was performed using ChemBET 3000 chemisorb instrument from Quantachrome. The effluent stream was monitored continuously with a thermal conductivity detector to determine the rate of ammonia desorption.

The steam stability of the sample was tested by treating 1 g of the calcined sample in the flowing water vapor at 600 °C for 4 h.

The reaction of 1, 2, 4-trimethylbenzene was carried out using a continuous fixed bed reactor at a reaction temperature of 400 °C and a weight hourly space velocity (WHSV) of 0.4/h. The catalyst amount is 0.5 g. The collected products were analyzed using GC with a capillary column of PEG-20 M and a flame ionization detector. The time on stream is 10 h. The results were compared with HMCM-41 and HZSM-5.

The amount of coke was determined by a thermogravimetric analyzer (Mettler Toledo TGA/SDTA 851$^e$). The used sample of 12 mg was heated in air from room temperature to 800 °C at a heating rate of 10 °C/min.

## 3 Results and Discussion

### 3.1 X-ray Diffraction

Figure 1 shows the small-angle X-ray diffraction patterns of AlKIT-1. The sample shows two peaks in $2\theta = 2$–5°, which can be indexed to (100) and (200) reflections associated with KIT-1 [4]. The (100) peak reflects a d spacing of 4.46 nm. After calcination in air at 550 °C for 6 h the

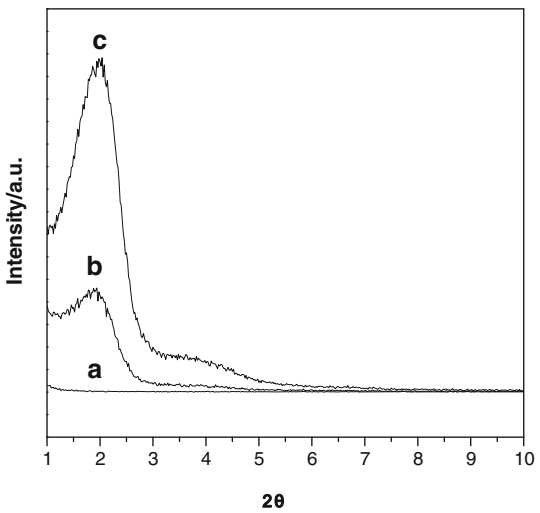


**Fig. 1** XRD patterns of **a** the empty sample holder, **b** as-synthesized nano-AlKIT-1, **c** calcined nano-AlKIT-1

peak intensities significantly increase, suggesting that the calcination and template desorption improve the structure ordering of the sample.

### 3.2 Transmission Electron Microscopy and Scanning Electron Microscopy

Figures 2 and 3 exhibit the TEM and SEM images of the calcined AlKIT-1, respectively. The TEM image of the sample (Fig. 2) shows that the pore structure is a three-dimensional, disordered network of short wormlike channels. This is the typical architectural feature of the framework of KIT-1 [4]. Furthermore, the TEM and SEM images (Fig. 3) show that the conglomerate particles have the sphere-like shape and the particle size is about 60–100 nm.

### 3.3 Adsorption Isotherms

$N_2$ adsorption–desorption isotherms of the samples are depicted in Fig. 4a. The adsorption and desorption curves of nano-KIT-1 and HMCM-41 exhibit a typical type-IV isotherm. The hysteresis loops are indicative of capillary condensation of $N_2$ inside mesoporous structures. The sharp inflection at $p/p_0 = 0.25$–$0.35$ on the isotherms of the untreated KIT-1 and HMCM-41 indicates the narrow uniform mesopore distribution (see Fig. 4b). After the steam treatment the slope of nano-KIT-1 becomes gentle and the pore size distribution becomes broader. The treatment leads to a decrease in average mesopore size of nano-KIT-1 from 2.7 to 2.4 nm. The nanosized AIKIT-1 retains 74% of the surface area and 83% of the pore volume after steaming, indicating its good steam stability.

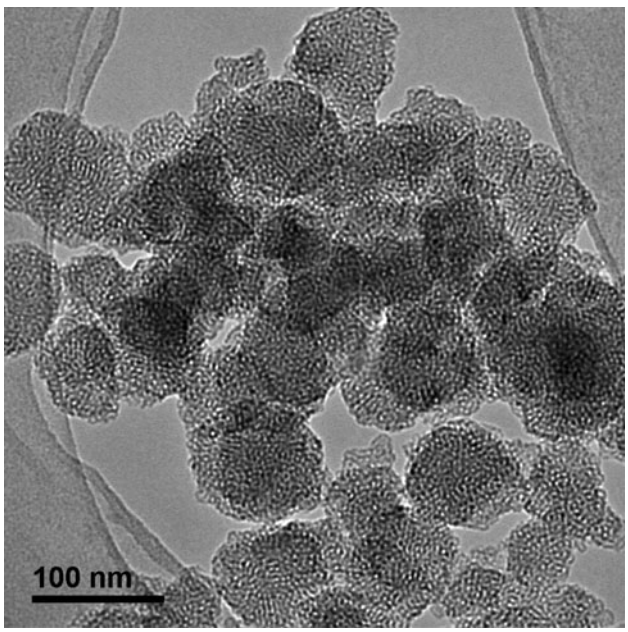


**Fig. 2** TEM image of calcined nano-AlKIT-1

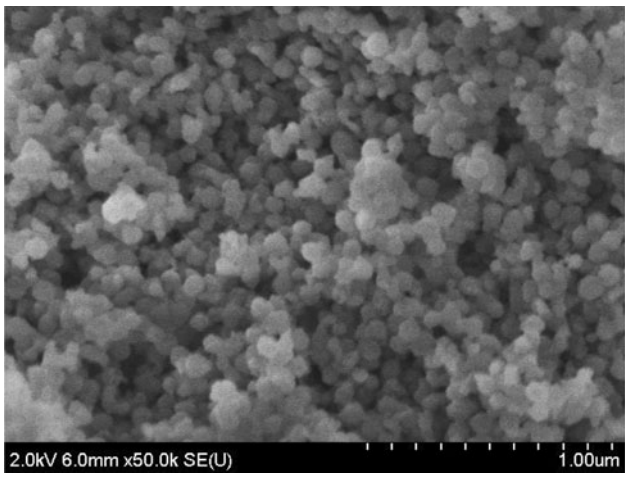


**Fig. 3** SEM image of calcined nano-AlKIT-1

Another step on the isotherms of nano-KIT-1 is observed in the adsorption curve at a relative pressure 0.9–1.0, which due to the filling of the macropore caused from the void space between the nanoparticals. Figure 4b and Table 1 show macropore size distribution of nano-KIT-1 at the mean values of 50 nm. By contrast, the HMCM-41 shows single narrow pore size distribution at the mean values of 2.4 nm.

Figure 4a illustrates the $N_2$ adsorption and desorption isotherms at 77 K of HZSM-5 sample. The adsorption at low relative pressures corresponds to the filling of micropore. The HK pore size distribution is shown in Fig. 4c. The BET surface area, pore size and pore volume of all samples are shown in Table 1.

### 3.4 Acid Properties

Figure 5 shows $NH_3$-TPD curves of the nano-AlKIT-1, HMCM-41, and HZSM-5. Evidently, the desorption temperature for ammonia on HZSM-5 is higher than that on nano-AlKIT-1 and HMCM-41, indicating that the acidic strength of HZSM-5 are much stronger than those of nano-AlKIT-1 and HMCM-41. The peak intensities of HZSM-5 are much higher than those of nano-AlKIT-1 and HMCM-41, suggesting that HZSM-5 has much more amount of acid sites. Obviously, the desorption peak of the nano-AlKIT-1 in the low temperature range is larger than that of HMCM-41. This indicates that the nano-AlKIT-1 has more weak acidic sites than the HMCM-41. However, the amount of the strong acidic sites cannot be compared because the desorption curve of the HMCM-41 does not go down to the base line. This result is repeatable. This may cause from further desorption of the hydroxyl groups from the mesoporous materials [7].

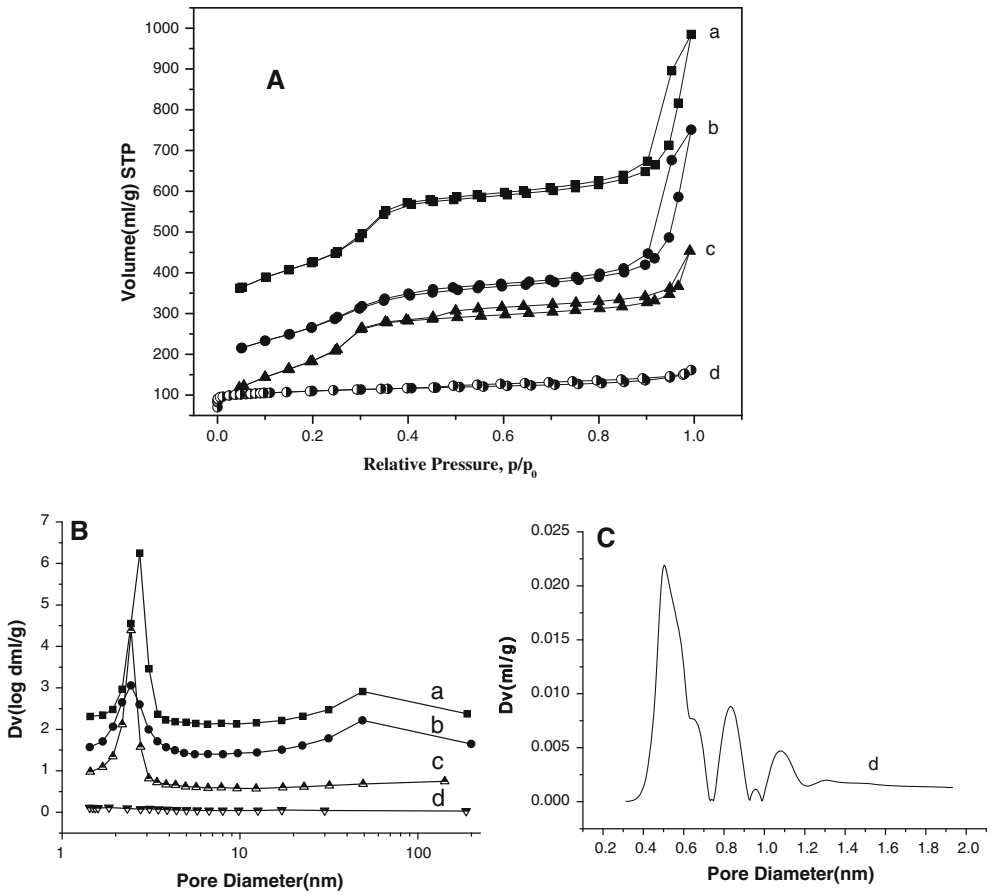


**Fig. 4** **a** Nitrogen adsorption disorption isotherm. **b** BJH pore size distribution. **c** HK pore size distribution. *a* calcined nano-AlKIT-1 *b* Nano-AlKIT-1 after treatment with 100% water steam at 600 °C for 4 h. *c* HMCM-41. *d* HZSM-5

**Table 1** Textural properties of the samples

| Catalysts | $SiO_2$/$Al_2O_3$ (mol%) | Surface area ($m^2$/g) | Pore size (nm) | Pore volume (mL/g) |
|---|---|---|---|---|
| Nano-AlKIT-1 | | | | |
| Before steaming | 63 | 822 | 2.7 and ~ 50 | 1.21 |
| After steaming | – | 612 | 2.4 and ~ 50 | 1.01 |
| HMCM-41 | 61 | 820 | 2.4 | 0.76 |
| HZSM-5 | 30 | 420 | 0.5–1.2 | 0.25 |

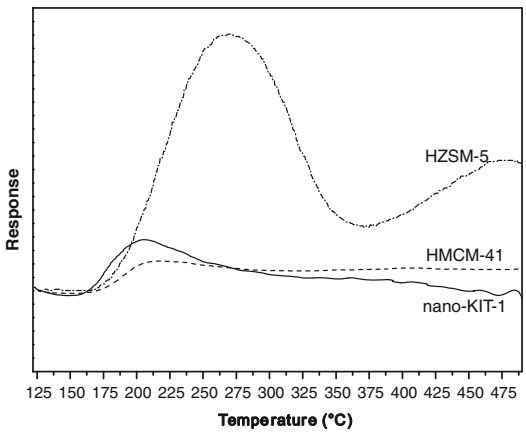


**Fig. 5** $NH_3$-TPD profiles of nano-AlKIT-1, HMCM-41, and HZSM-5

## 3.5 Catalytic Property

The catalytic activities of the nano-AlKIT-1, HMCM-41, and HZSM-5 for 1,2,4-trimethylbenzene transformation are illustrated in Table 2. As shown in Table 2, the catalytic activity for the AlKIT-1 is higher than that of the HMCM-41 and HZSM-5. Not only the three-dimensional wormlike pore channels of the nano-AlKIT-1 with the secondary pores are more beneficial to the diffusion and transport of reactants and products in catalytic reactions as compared to one-dimensional channels of the HMCM-41, but also the nano-AlKIT-1 has more weak acidic sites than the HMCM-41. Although HZSM-5 shows strong acidity, its lower activity for 1,2,4-trimethylbenzene transformation is due to

**Table 2** Catalytic performance of different catalysts for 1,2,4-trimethylbenzene (wt%)

| Catalysts | Reaction time (h) | $C_{1,2,4\text{-TMB}}$(%) | Main product distribution (%) | | | | | |
|---|---|---|---|---|---|---|---|---|
| | | | Toluene | Xylenes | 1,3,5-TMB | 1,2,4-TMB | 1,2,3-TMB | TetraMBs |
| Nano-AlKIT-1 | 6 | 46.5 | 0.3 | 11.7 | 16.1 | 52.8 | 6.3 | 12.8 |
| | 8 | 45.1 | 0.2 | 10.8 | 15.9 | 54.3 | 6.5 | 11.9 |
| | 10 | 42.8 | 0.2 | 9.9 | 15.4 | 56.7 | 6.6 | 11.0 |
| HMCM-41 | 6 | 13.9 | 0.1 | 3.0 | 4.8 | 85.2 | 3.2 | 3.4 |
| | 8 | 12.6 | 0.1 | 2.8 | 4.3 | 86.6 | 2.9 | 3.1 |
| | 10 | 11.5 | 0.1 | 2.5 | 3.9 | 87.6 | 2.7 | 2.9 |
| HZSM-5 | 6 | 32.1 | 2.5 | 11.3 | 12.8 | 67.2 | 5.2 | 0.5 |
| | 8 | 31.1 | 2.9 | 11.0 | 11.8 | 68.2 | 5.0 | 0.5 |
| | 10 | 30.0 | 2.6 | 11.0 | 11.2 | 69.3 | 4.8 | 0.4 |

its relatively small pore size and the large diameter of the reactant molecules.

In this system, isomerization, dealkylation, and disproportionation of 1,2,4-TMB and other secondary reactions occur. Table 2 gives the main products of 1,2,4-trimethylbenzene transformation. The different distribution of products is due to the different acid sites and pore structures. For the nano-AlKIT-1, the yields of the isomerization and disproportionation products are almost same. The formation of a small amount of the cracking products (toluene, benzene, and light hydrocarbon components) suggests that nano-AlKIT-1 has a certain amount of strong acid sites, because the cracking reaction needs stronger acid sites than the isomerization reaction [12]. As for the HMCM-41, the yield of isomerization products is higher than that of disproportionation products. This is because disproportionation needs stronger acid sites than isomerization and the isomerization of 1,2,4-TMB is a fast reaction which occurs on the external surface [13–16]. Furthermore, the absence of the cracking products indicates that HMCM-41 possess little strong acid centers. In contrast, the HZSM-5 possesses strong acidic sites, which leads to large amount of the cracking products. However, the small channels ($\sim$0.5 nm) make 1,2,4-TMB (0.74 nm) difficult to diffuse effectively in the pore system. Only the acid sites on the external surface and pore mouth contribute to the reactions.

The TG analysis results show that after 10 h run, the amounts of coke formation on the nano-KIT-1, HMCM-41, and HZSM-5 are 8.2, 7.5, and 4.7%. The data in Table 2 shows that the amount of tetramethylbenzenes produced on nano-KIT-1 is higher than those on HMCM-41 and HZSM-5. This indicates that the pores of nano-KIT-1 are spacious enough to allow the bulky aromatics to diffuse freely. The possibility to produce bulky aromatic molecules, which are the precursor of coke, is increased. However, nano-KIT-1 still shows higher activity than HMCM-41 and HZSM-5, indicating that nano-KIT-1 has a very good ability to tolerate the coke deposits. This is because the secondary pores of nano-KIT-1 accommodate the coke deposits, delaying the blocking of the channel by coke. Therefore, nano-AlKIT-1 shows good catalytic performance for 1,2,4-TMB due to its unique pore channels structure and acid strength.

## 4 Conclusions

We have developed a simple synthetic route for preparing nanosized AlKIT-1 molecular sieve. The nanosized AlKIT-1 has hierarchical pore structure and medium acid strength, and exhibits good hydrothermal stability. The sample shows better catalytic performance in the conversion of 1,2,4-trimethylbenzene than HMCM-41 and HZSM-5. These results indicate that the nanosized AlKIT-1 offers new opportunity for the conversion of large molecules.

**Acknowledgments** This study was financially supported by the National Science Foundation of China (NSFC, Grant 20773019, 20603004) and the National "973" Project of China (2011CB201301).

## References

1. Kresge CT, Leonowicz ME, Roth WJ, Wartuli JC, Beck JS (1992) Nature 359:710
2. Tanev PT, Pinnavaia TJ (1995) Science 267:865
3. Bagshaw SA, Prouzet E, Pinnavaia TJ (1995) Science 269:242
4. Ryoo R, Kim JM, Ko CH, Shin CH (1996) J Phys Chem 100:7718
5. Zhao DY, Feng JL, Huo QS, Melosh N, Fredrickson GH, Chmelka BF, Stucky GD (1998) Science 279:48
6. Jun S, Ryoo R (2000) J Catal 195:237
7. Zhao DY, Nie C, Zhou YM, Xia SJ, Huang LM, Li QZ (2001) Catal Today 68:11
8. Yue YH, Sun Y, Gao Z (1997) Catal Lett 47:167
9. Tosheva L, Valtchev VP (2005) Chem Mater 17:2494
10. Selvin R, Hsu HL, Her TM (2008) Catal Commun 10:169

11. Ji XF, Qin ZF, Dong M, Wang GF, Dou T, Wang JG (2007) Catal Lett 117:171
12. Wang KY, Wang XS (2008) Micropor Mesopor Mater 112:187
13. Morin S, Ayrault P, Mouahid SE, Gnep NS, Guisnet M (1997) Appl Catal A Gen 159:317
14. Ratnasamy P, Sivasankar S, Vishnoi S (1981) J Catal 69:428
15. Molina R, Schutz A, Poncelet G (1994) J Catal 145:79
16. Roger HP, Moller KP, O'Connor CT (1998) J Catal 176:68